Structural Properties of Complex Plasmas in a Homogeneous dc Discharge

S. Mitic, B. A. Klumov, U. Konopka, M. H. Thoma, and G. E. Morfill
Max-Planck-Institut für Extraterrestrische Physik, D-85741 Garching, Germany
(Received 9 April 2008; published 16 September 2008)

We report on the first three-dimensional (3D) complex plasma structure analysis for an experiment that was performed in an elongated discharge tube in the absence of striations. The low frequency discharge was established with 1 kHz alternating dc current through a cylindrical glass tube filled with neon at 30 Pa. The injected particle cloud consisted of monodisperse microparticles. A scanning laser sheet and a camera were used to determine the particle position in 3D. The observed cylindrical-shaped particle cloud showed an ordered structure with a distinct outer particle shell. The observations are in agreement with performed molecular dynamics simulations.

DOI: 10.1103/PhysRevLett.101.125002 PACS numbers: 52.27.Lw

Since the discovery of plasma crystals, many experiments have been performed to quantify the crystalline state of complex plasmas by means of analyzing the scattered laser light of the microparticles that were introduced in the plasma environment. Most of these experiments were related to two-dimensional (2D) systems (e.g., [1–5]). Only a few experiments were focused on the analysis of 3D structures [6–14]. Extensive analysis on the crystallization phase transition by means of structural properties of a substantial particle cloud has been performed for 2D—[3] as well as 3D [12]—particle systems in radio-frequency discharges (the analysis of the 3D particle system was based on a 2D cross section analysis). A full 3D reconstruction has so far been reported only for systems smaller than a few hundred particles [10,15]. For dc discharges, crystalline systems have been investigated only in striations [8] or in double dc-plasma environments [16]. However, a full 3D structure analysis of these systems has not been performed.

Here we present for the first time a full 3D reconstruction of a microparticle cloud in a low frequency discharge plasma. In contrast to typical complex plasma experiments in dc discharge tubes [8], the particles in the experiment described here were not levitated in striations, where strong variations in the electric field lead to inhomogeneities in particle clouds even on small scales. Instead, the particles were confined in a horizontally mounted discharge tube, levitated by the radial electric field of the plasma sheath that was aligned with the tube walls. The discharge conditions were selected in a way that no striations were present in the positive column. In this way, large homogeneous particle clouds could be established.

The experiment setup was similar to the dc discharge experiment facility "PK-4" [17] that is being developed for complex plasma microgravity experiments aboard the International Space Station. The heart of the setup was given by a "*U*"-shaped discharge glass tube as sketched in Fig. 1. The discharge tube was filled with Ne at a pressure of 30 Pa using a flow controller for gas inlet on one side of the tube and a vacuum pump on the other side. For stability reasons, the gas inlet as well as the pump could be disconnected by valves so that experiments without gas flow but with stable discharge conditions could be performed. The stability period was about 10 minutes with closed valves. After this time, gas refreshment was necessary to avoid plasma parameter drift.

To ignite a plasma, a voltage of about 1000 V was applied along the discharge tube between the driven electrodes. This corresponded in our case to a dc current of 1 mA through the plasma. Under these circumstances, a longitudinal electric field is present in the discharge accompanied by a substantial directed ion flow. Since charged microparticles react to the electric fields as well as the ion flow, no steady-state conditions for microparticles introduced in the discharge can be reached in such a case. To compensate the effects of the longitudinal electric

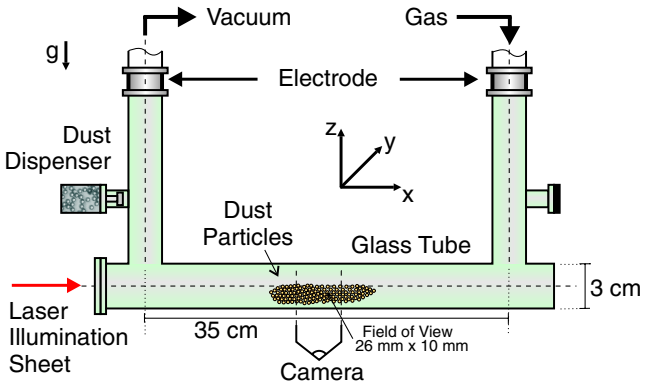

FIG. 1 (color online). Experimental setup. The tube had an inner diameter of 30 mm and a length of 750 mm with electrodes on both ends. The part of the discharge tube that was aligned perpendicular to the gravity vector had a length of about 350 mm with flat windows at the sides for optical illumination and observation purposes. To assure clean gas conditions, the discharge tube was always evacuated for several hours before each experiment, reaching base pressures below 10^{-3} Pa.

fields on particles in the plasma, the polarity of the voltage between the electrodes was switched with a frequency of 1 kHz. This frequency is far above the response frequency of the "heavy" microparticles in the experiments, so that the particles "see" a time-averaged zero longitudinal electric field and ion flow.

The particle cloud consisted of monodisperse, spherical melamine formaldehyde micron-sized particles of radius $r_p = (2.4 \pm 0.1)\ \mu$m and mass density $\rho_p = 1.51\ \mathrm{g/cm^3}$. The particle injection was via a dispenser mounted on one side of the glass tube. By changing the duty cycle of the polarity-switched plasma current, a time-averaged net force along the tube can be set. As a result, the particle cloud can be moved to any desired position within the tube. Our experiments were conducted with the particle cloud in the center of the discharge tube which was horizontally aligned. The particle cloud is then confined by the radial electric field of the sheath as well as horizontally by a weak confinement potential caused by the bends in the glass tube on both sides. The overall shape of the particle cloud represented the confinement structure in the discharge tube. The thickness and density of the cloud was higher in its center, while its size reduced to a few layers or even a single particle string at both ends. Typical length of the dust cloud was about 10 cm.

The particles were illuminated by a horizontally aligned sheet of laser light with a power of ~20 mW at a wavelength of 686 nm. The minimal thickness of the illumination sheet was about $\delta_L = (150 \pm 30)\ \mu$m. The positions of the particles were recorded with 50 frames per second by a camera that had a field of view of 26 mm along the tube and 10 mm across it.

Both camera and laser were attached to a translation stage that allowed for scans in height with a constant velocity while keeping the relative positions of camera and laser sheet fixed. The optimal scanning velocity was found to be 0.2 cm/s for two reasons. First, the velocity has to be low enough that the same particles appear at least in a few consecutive frames of the scan, and, second, the particle motion time (changes in 3D structure) is large compared to the scanning time. To determine the full spatial position of each particle, every particle position within each frame of a scan was identified. Using a correlation analysis, corresponding particles in consecutive frames were identified, and from these particle tracks the three-dimensional particle positions were calculated using the (light) intensity weighted x and y positions and frame number, which is related by the scanning velocity with the z coordinate. This diagnostic method has been also used in our group by Zuzic *et al.* [7].

After injection of the particles and positioning of the particle cloud, the particles within the cloud did not have a well defined arrangement; i.e., the cloud was in a disordered state. A few minutes later, the first layers started to separate in the upper part of the particle cloud. About 10 minutes after injection, the system showed a partly ordered structure. At this time, a scan was performed shortly before the gas refreshment cycle that would destroy the structure of the particle system. The three-dimensional positions of the particles in the observed part of the cloud are presented in Fig. 2. Particle positions are overlaid for all microspheres in the cloud showing the projection of the system in the side view and top view (images in Fig. 2, upper part and lower part, respectively). As can be clearly seen, the particles in the bulk of the cloud represent a kind of vertically orientated structure with a single distinct outer particle layer that represented the structure of the radial confinement across the discharge tube.

To be able to compare the structural properties with molecular dynamics (MD) simulations, we had to estimate the corresponding experiment parameters. Using plasma parameter measurements from Ref. [18] (obtained using the same experimental setup), we estimate for the pressure of 30 Pa and the discharge current of 1 mA an electron and ion density of $n_e \approx n_i \approx 10^8\ \mathrm{cm^{-3}}$, an electron temperature of $T_e \approx 6$ eV, and an ion temperature of $T_i \approx 0.03$ eV. The corresponding characteristic length scales were $\lambda_D = 120\ \mu$m for the combined Debye length ($\lambda_D = 1/\sqrt{1/\lambda_{De}^2 + 1/\lambda_{Di}^2}$, where subscript e stands for electron and i for ion) and $\lambda_{imfp} = 180\ \mu$m for the ion mean free

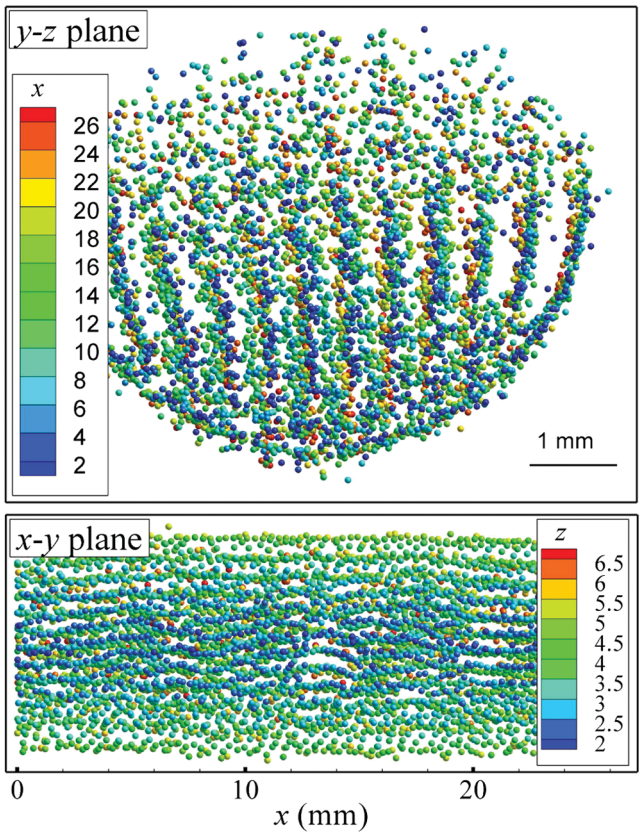

FIG. 2 (color). Experimentally recorded particle positions in the y-z and x-y planes (see orientation in Fig. 1). Particles are color-coded by corresponding third coordinate presented in millimeters. About 6000 particles were detected.

path. Using a 3D pair correlation analysis, we obtained for the interparticle distance $\Delta \approx 500\ \mu$m. From the "orbit motion limited" equation [19] and taking into account a correction for the charge reduction as obtained in Ref. [20] for the ratios $r_p/\lambda_D \approx 0.02$ and $\lambda_D/\lambda_{imfp} \approx 0.7$, we estimated the charge of the particles to have been $Z_d \simeq 5 \times 10^3$ electrons. As a result, we could calculate the coupling parameter $\Gamma \simeq 10$, using the definition $\Gamma = Z_D^2 \exp(-k)/\Delta T_d$, where $k = \Delta/\lambda_D \approx 4$. This would theoretically represent a liquid state.

For the molecular dynamic simulations, we assumed that all microparticles have the same charge $Z_d = 3 \times 10^3 e$, where e is the electron charge, and the pair interaction between the particles is described by a screened Coulomb (Yukawa) potential $\phi(r) = Z_d/r \exp(-r/\lambda_D)$, with r the distance between the particles and λ_D the screening length. The system of equations

$$m\ddot{\mathbf{r}}_i = -Z_d \sum \nabla\phi - m\gamma\dot{\mathbf{r}}_i - m\mathbf{g} + \mathbf{L}_i \qquad (1)$$

was solved for each particle using the standard Verlet algorithm, where γ describes Epstein friction. The terms on the right-hand side of Eq. (1) describe the electrostatic interaction between particles, neutral drag, gravity, and the stochastic Langevin force (thermal noise induced by particle collision with the neutral gas) defined from $\langle \mathbf{L}_i(t)\mathbf{L}_j(t+\tau)\rangle = 2\gamma m k_B T \delta_{ij}\delta(\tau)$, with the zero-mean condition $\langle \mathbf{L}_i(t)\rangle = 0$ (e.g., [21]).

Initially $N = 6000$ particles were randomly distributed over a cylinder of radius $r_c \sim 1$ cm. Periodical boundary conditions along z and parabolic confinement in the x-y plane were used. The parameters were similar to those of the experiment (particle size, mean interparticle distance Δ, neutral gas density). Figure 3 shows typical particle positions at the steady-state stage for $\Gamma \simeq 10$.

3D particle positions can be used to define the local order of particles, which in turn gives us the key information about the phase state of the system to be investigated.

To determine the local order of the particles, a bond order parameter method is used [22]. In the framework of this method, the local rotational invariants for each particle

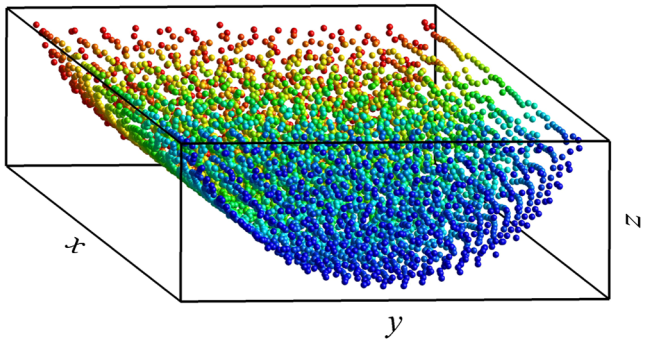

FIG. 3 (color online). MD simulations of the Yukawa system of dust particles. Snapshot of particle positions at steady-state stage.

are calculated and compared with those for ideal lattice types such as fcc/hcp/bcc. Local rotational invariants of second order $q_l(i)$ and third order $w_l(i)$ are calculated for each particle i by using $N_b(i)$ nearest neighbors:

$$q_l(i) = \left(\frac{4\pi}{(2l+1)} \sum_{m=-l}^{m=l} |q_{lm}(i)|^2\right)^{1/2}, \qquad (2)$$

$$w_l(i) = \sum_{\substack{m_1,m_2,m_3 \\ m_1+m_2+m_3=0}} \begin{bmatrix} l & l & l \\ m_1 & m_2 & m_3 \end{bmatrix} q_{lm_1}(i) q_{lm_2}(i) q_{lm_3}(i), \qquad (3)$$

where $q_{lm}(i) = \frac{1}{N_b(i)} \sum_{j=1}^{N_b(i)} Y_{lm}(r_{ij})$ and Y_{lm} are the spherical harmonics and $r_{ij} = r_i - r_j$, where r_i are the coordinates of ith particle. In Eq. (3),

$$\begin{bmatrix} l & l & l \\ m_1 & m_2 & m_3 \end{bmatrix}$$

are the Wigner $3j$ symbols, and the summation in the latter expression is performed over all indices $m_i = -l, \ldots, l$, that satisfy the condition $m_1 + m_2 + m_3 = 0$.

To define the local order around a particle, we used q_4, q_6, and w_4. Figure 4 shows the simulated distributions of a Yukawa system of particles in the $q_4 - q_6$ plane for a liquidlike system ($\Gamma \sim 1$) [Fig. 4(b)] and a crystallized one ($\Gamma \simeq 10^4$) [Fig. 4(a)]. Results of the experiment are

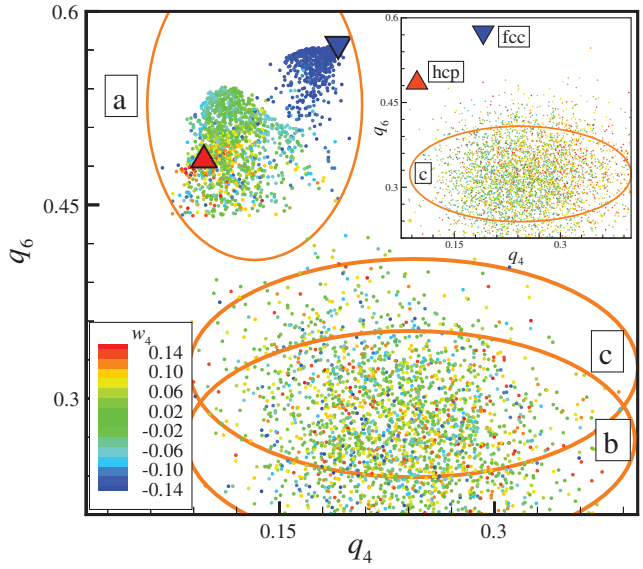

FIG. 4 (color). Distribution of dust particles at different values of Γ in the plane of local order parameters $q_4 - q_6$ (calculated by using 12 nearest neighbors) as seen from MD simulations of Yukawa systems of particles together with experimental data. Scattered data are color-coded by the third-order rotational invariant w_4 value. Data for ideal hcp ($\triangle$) and fcc (∇) are also plotted. Distribution (b) shows liquidlike system with $\Gamma \sim 1$, while case (a) corresponds to a crystallized Yukawa system with $\Gamma \simeq 10^4$. Experimental data are scattered within the area marked with (c) and in detail presented in the inset.

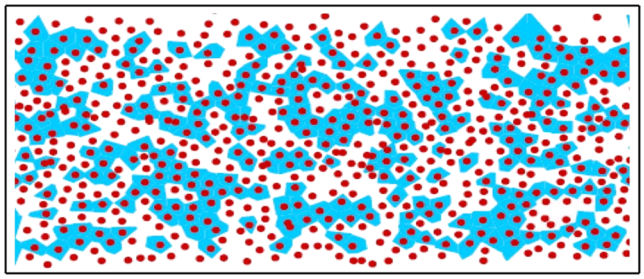

FIG. 5 (color online). Particle arrangement in the unfolded outer shell representation where shaded areas represent particles with 6 nearest neighbors.

plotted revealing liquidlike behavior of the observed data [Fig. 4(c)]. To obtain the crystallized Yukawa system, we performed 3D MD simulations of 6000 particles in a box with external confinement of a hard wall type in the vertical direction (z) with periodic boundary conditions in the horizontal (x and y) directions.

From both projections presented in Fig. 2, some macrostructures are visible. In the y-z projection, formation of layers is very well pronounced. In the central part of the cloud, layers are parallel, while on the ends in the radial direction they are curved following the shape of the confinement. Outer particles form a shell structure around these layers, and the shape of this shell is strongly dependent on the plasma confinement and particle number [23]. In a first step, the shell was unfolded, and then a triangulation and Voronoi analysis were done. The particle arrangement in this unfolded shell was analyzed, and the results are presented in Fig. 5. The shaded area around the particles represents particles which have 6 nearest neighbors, and they make up about 50% of all particles in this shell. About 25% of all particles have 5 neighbors, and about 20% have 7 neighbors. For a 2D plane, a sixfold structure represents the ground state in the crystal state, so the percentage of the sixfold structure can be used for the determination of the coupling parameter Γ [24]. By comparing this results with simulations [24], the value of Γ in this measurement is estimated to be about 10, which is consistent with our independent estimations based on the plasma parameters.

In this Letter, we presented the first 3D analysis of a complex plasma in a dc discharge environment. The discharge was switched at a rate of 1 kHz to produce striation-free plasma. The 3D analysis of the particle cloud showed a liquidlike structure with locally enhanced structural properties that indicated that the system was near crystallization. Molecular dynamics simulations were performed taking into account the experimental conditions. The simulated and experimental results were analyzed using methods to quantify the dynamical properties of liquidlike or glassy systems. Simulation and experiment showed good agreement. In addition, both showed a transition of a more structural particle arrangement from the outside of the particle cloud to a more irregular arrangement on the inside. On the outside, a shell-like structure could be observed. This could be of special interest, since it suggests that physical properties such as the shear viscosity might be anisotropic. The observed shell structure does not contradict the liquid behavior of the system, since it consists of only a few layers corresponding to a real liquid on the nanoscale. Thus confined complex plasma systems might help us to understand similar generic properties of other cylindrical-shaped systems, particularly those on the nanometer scale.

We acknowledge the support of DLR under Grants No. 50 WM 0504 and No. 50 WP 0700.

[1] H. M. Thomas and G. E. Morfill, J. Vac. Sci. Technol. A **14**, 501 (1996).
[2] G. E. Morfill, H. M. Thomas, U. Konopka, and M. Zuzic, Phys. Plasmas **6**, 1769 (1999).
[3] C. A. Knapek *et al.*, Phys. Rev. Lett. **98**, 015004 (2007).
[4] V. Nosenko, S. Zhdanov, and G. Morfill, Phys. Rev. Lett. **99**, 025002 (2007).
[5] A. Melzer, Phys. Rev. E **67**, 016411 (2003).
[6] Y. Hayashi, Phys. Rev. Lett. **83**, 4764 (1999).
[7] M. Zuzic *et al.*, Phys. Rev. Lett. **85**, 4064 (2000).
[8] V. E. Fortov *et al.*, in *Dusty Plasmas in the New Millenium: Third International Conference on the Physics of Dusty Plasmas* (AIP, New York, 2002).
[9] Y. Hayashi, in *Non-Neutral Plasmas Physics IV* (AIP, New York, 2002).
[10] O. Arp, D. Block, A. Piel, and A. Melzer, Phys. Rev. Lett. **93**, 165004 (2004).
[11] M. H. Thoma *et al.*, Am. J. Phys. **73**, 420 (2005).
[12] M. Rubin-Zuzic *et al.*, Nature Phys. **2**, 181 (2006).
[13] A. P. Nefedov *et al.*, New J. Phys. **5**, 33.1 (2003).
[14] G. E. Morfill *et al.*, in *Dusty Plasmas in the New Millenium: Third International Conference on the Physics of Dusty Plasmas*, AIP Conf. Proc. No. 649, edited by R. Bharuthram, F. Verheest, P. K. Shukla, and M. A. Hellberg (AIP, New York, 2002), p. 91.
[15] T. Antonova *et al.*, Phys. Rev. Lett. **96**, 115001 (2006).
[16] N. Sato, G. Uchida, R. Ozaki, and S. Lizuka, in *Physics of Dusty Plasmas* (AIP, New York, 1998).
[17] M. H. Thoma *et al.*, IEEE Trans. Plasma Sci. **35**, 255 (2007).
[18] V. E. Fortov *et al.*, Plasma Phys. Controlled Fusion **47**, B537 (2005).
[19] T. Matsoukas and M. Russell, J. Appl. Phys. **77**, 4285 (1995).
[20] B. Rovagnati, M. Davoudabadi, G. Lapenta, and F. Mashayek, J. Appl. Phys. **102**, 073302 (2007).
[21] B. Smit and D. Frenkel, *Understanding Molecular Simulation* (Academic, San Diego, 2002).
[22] P. Steinhardt, D. Nelson, and M. Ronchetti, Phys. Rev. Lett. **47**, 1297 (1981).
[23] Shell-like structures in complex plasmas have also been observed in an rf discharge, where a limited number of microparticles was spherically confined [10].
[24] B. A. Klumov and G. E. Morfill, JETP Lett. **85**, 498 (2007).